AI-Assisted Drone Surveys for Mojave Desert Tortoises within the Boulder City Conservation Easement, Clark County, NV: 2025 Season

Report submitted to
Desert Conservation Program
Clark County

Matthew Bandy
Resi Solutions

Resi-2025-036-01
July 2025

AI-Assisted Drone Surveys for Mojave Desert Tortoises within the Boulder City Conservation Easement, Clark County, NV: 2025 Season

Report submitted to Clark County Desert Conservation Program

Matthew Bandy

July, 2025

Resi-2025-036-01

Resi Solutions

Executive Summary

This report describes an AI-assisted drone survey for Mojave desert tortoises conducted between April 15 and May 10, 2025. The study area was composed of a series of eight widely spaced 500 acre monitoring plots within the Boulder City Conservation Easement (BCCE) in Clark County, NV. Approximately 4,080 acres were subjected to low altitude photography using a drone during the period in which the animals were active above ground. A computer vision model was used to detect tortoises and tortoise soil burrows in the acquired imagery.

- Ten adult tortoises (Midline Carapace Length [MCL] >= 180 mm) were detected in the survey area, as well as five subadults/juveniles and ten tortoise carcasses. Fifty active or intact tortoise burrows were also detected.
- Adult tortoise density in the surveyed area was estimated to be 2.9 tortoises/km^2 with a 90% confidence interval between 2.3 and 3.5 tortoises/km^2. Tortoise abundance in the BCCE as a whole was estimated to be 1025 with a 90% confidence interval between 825 and 1219, based on a sample acreage of 4.7% of the easement.
- Improved drone and camera options employed in this survey resulted in a significant improvement in detection rates and speed of data acquisition, making possible a successful survey in very challenging conditions.

Contents

List of Figures

List of Tables

1. Introduction

Small unmanned aerial vehicles (sUAS, or "drones") are becoming an important tool for wildlife biology, especially for population monitoring (e.g. Augustine and Burchfield 2022; Christie et al. 2016; Delplanque et al. 2021; Elmore et al. 2021; Huerta et al. 2020; Hyun et al. 2020; Inman et al. 2019; Jones et al. 2006; Linchant et al. 2018; Ramos et al. 2018; Watts et al. 2008; Zhou et al. 2021). Recent work conducted by Resi has shown that drone surveys can be an effective means of studying tortoise populations in the deserts of western North America (Bandy 2021, 2022; Bandy and Rognan 2022).

Between March 15 and May 10, 2025, Resi and Bio Logical, LLC partnered to conduct a drone survey within the Boulder City Conservation Easement (BCCE) in Clark County, NV (Figure 1.1). This work was conducted under contract to the Clark County Desert Conservation Program. The goal of the survey was to measure Mojave desert tortoise (*Gopherus agassizii*) occupancy within eight 500-acre survey plots scattered throughout the project area. Matthew Bandy piloted the drone under contract to Bio Logical. Dan Roadhouse was Bio Logical's project manager. Flights were conducted between two hours after sunrise and 1 PM daily. Flights began on April 15 and ended on May 10, and were suspended on days when the weather was too cold for tortoise surface activity to be expected.

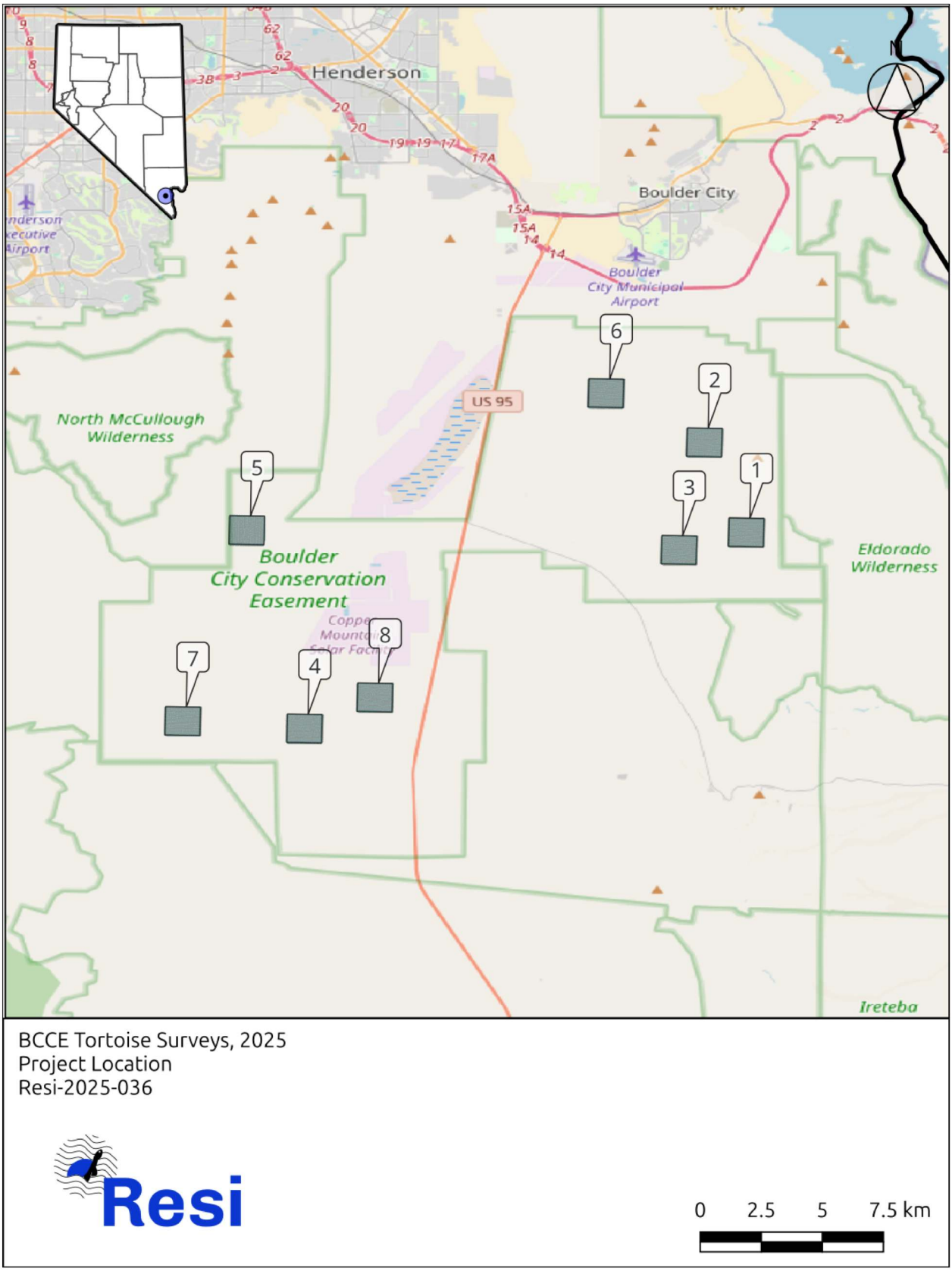

Figure 1.1. Project location map

2. Methods and Materials

The drone survey method, the use of convolutional neural networks for tortoise detection in drone photos, and Resi's bespoke implementation of distance sampling methods to generate density and abundance estimates from these detections, is described in detail in Chapter 2 of Bandy (2022). The reader is referred to that document for a detailed treatment. The method will be described in only general terms below.

2.1. Drone Flights

This season, Resi employed a new hardware platform consisting of a domestically produced aircraft and a higher-quality and higher-resolution camera. The drone used was a Freefly Astro fitted with the Sony Apha 7R IV 61 megapixel camera and a 50 mm lens. Flight planning and execution was performed using the Auterion Mission Control application. Matthew Bandy of Resi planned the flights and piloted the aircraft. The target ground sample distance (GSD) was 5.5 mm. Previous work (Bandy 2024a) has shown that 73 meters is the optimal flight elevation for the detection of adult Mojave desert tortoises using the selected hardware and software in the Mojave desert environment. All flights conducted as part of this survey were flown at 73 meters flight elevation. Terrain-following methods were employed to maintain a constant height above ground.

Flights were planned to cover a total of eight 500-acre tortoise sample plots within the greater conservation easement (Figure 1.1). Drone flights, however, typically photographed a somewhat larger area due to photo boundaries extending beyond the plot footprint. The area photographed for a fully surveyed plot was approximately 505-514 acres, as show in Appendix A. Each plot was flown three times over the course of three survey periods, each consisting of five days of flying. Flights days were not necessarily continuous within a survey period, since cold weather days were skipped due to presumed very low tortoise detectability. The first survey period began on April 15, the second on April 23, and the third began on May 6 and ended on May 10 (Appendix A). Each survey period photographed a total area of approximately 4,077 acres, for a total survey effort of 12,230.1 acres photographed.

Tortoise survey flights were conducted between two hours after sunrise and 1 PM. Previous studies have shown that tortoise visibility to drone photography varies dramatically by time of day (Bandy and Rognan 2022: 17-20; Bandy 2023: 14-16). In particular, in the afternoons tortoises tend to be located in their burrows or under the shade of vegetation, where they may be visible to pedestrian surveyors but are invisible from the air. In the mornings, by contrast, the animals are much more likely to be actively foraging or in motion and not under cover. Drone surveys conducted in the afternoons are therefore largely ineffective.

2.2. Computer Vision

Photographs were processed by a computer vision model trained by Resi using the PyTorch framework (Paszke et al. 2019), an open source environment for creating and training convolutional neural networks (CNNs). All drone photographs collected in the course of this project were processed by Resi's CNN models and tortoise detections were tabulated and geolocated. All detections received a final review by a human observer. MCL was determined by measuring the length of the carapace on the photograph in pixels, then multiplying this quantity by the GSD of the photograph (for this project, 5.5 mm).

2.3. Distance Analysis

Distance sampling is a family of statistical methods that use observations of the distance of detections from an observer to estimate density and abundance of a population (Buckland et al. 2001; Thomas et al. 2010; Miller et al. 2013, 2017). Resi has developed DroneDistance: a novel implementation of point distance sampling that treats drone photographs as rectangular point samples. The DroneDistance R package was used to generate density and abundance estimates from raw tortoise detection data. The statistical methodology underpinning these calculations was first outlined in detail in Bandy (2022). That discussion is reproduced below.

2.3.1. The droneDistance R package

DroneDistance is an R package developed by Resi for distance sampling and analysis of aerial photographic datasets. It is an entirely novel implementation of the distance sampling methodology and shares no code with Distance 7.5 or its predecessors. Aerial photos are

conceptualized as point samples that are truncated at the photo boundary. That is to say that each photograph is a rectangular point sample and the distance to detections is measured from the center of the photograph (i.e. the location of the drone at the instant the photograph was taken). The package accounts for photo distribution and overlap in its estimation of detection rates. Inputs to the package are spatial datasets describing photo boundaries and detection locations. The DRONEDISTANCE workflow and statistical methodology is outlined in the following sections.

2.3.2. Fitting the distance model $g(r)$

In this step we fit a model describing the relationship between detection probability and distance from the center of the photograph. Photo data are read from *.csv* files with well-known text (WKT) polygons and points describing the boundary and center of each photograph measured in meters with a consistent coordinate system among all the photos (e.g., UTM coordinates from the same zone). Detection locations are read from a separate *.csv* with WKT points specifying detections. If an individual is detected more than once (e.g., in two intersecting photos), both detections are included in the *.csv*. However, one of the detections is identified as a duplicate in an additional column that gives F or FALSE for one of the detections and T or TRUE for the duplicate(s). The detections file must also include a column with unique identifiers for the photos in which they were detected, typically a globally unique identifier (GUID). Each unique identifier must have a corresponding entry in the photo polygons file.

The detection function is fit by maximum likelihood estimation, using Poisson regression of the number of detections as a function of the square of the distance from the center of the photograph. An offset term accounts for the area searched at each distance. The model requires that each photograph be split into a large number of concentric rings (100 by default), the area in each ring calculated, and the number of detections tallied.

The probability of detection ($g(r)$) is assumed to decrease with distance from the center (r) of the photograph as a half-normal probability density function (PDF), scaled so that $g(0) = 1$. The $g(0) = 1$ assumption is normally unrealistic, particularly when searching for cryptic taxa such as the desert tortoise, so it is scaled by g_0 in a subsequent step.

2.3.3. Estimation of g_r

The overall detection probability for individuals within a surveyed area is the integral of the distance function ($g(r)$,described above) over all the photographs with an adjustment

for the areas of photo intersection. Exact evaluation of the integral and the adjustment for intersections would involve intricate bookkeeping, which is difficult to code, debug, and maintain. As an alternative, DRONEDISTANCE approximates the integral by generating a large number (default is 10,000) of random locations in the coverage area, calculating $g(r)$ for each location and taking the average. Locations that are in a single photograph are assumed to have $g = g(r_{i,j})$, where $r_{i,j}$ is the distance between the location (i) and the center of photograph (j).

Locations (i) that are in the intersection of two photographs are assigned a detection probability of $\hat{g}(r) = 1 - (1 - \hat{g}(r_1))(1 - \hat{g}(r_2))$ where r_1 and r_2 are the distances from the center in photographs 1 and 2. Likewise, for a detection location in the intersection of three photographs, $\hat{g}(r) = 1 - (1 - \hat{g}(r_1))(1 - \hat{g}(r_2))(1 - \hat{g}(r_3))$.

Uncertainty is accounted for via simulation of the β parameter from the generalized linear model and transforming to g. More precisely, according to the asymptotic properties of maximum likelihood estimators, the distribution of the distance parameter is approximately $\hat{\beta} \sim n(\mu = \hat{\beta}, \sigma^2 = v\hat{a}r(\beta))$, and $\hat{g}(r) = e^{\hat{\beta}r^2}$.

2.3.4. Estimation of g_0

Detectability of individuals in the center of a photograph is estimated as $g_0 \sim beta(\alpha = x + 0.5, \beta = n - x + 0.5)$, where n is the total known individuals and x is an accurate count of whether the individuals would be detectable. This is the posterior distribution for the binomial p parameter, derived from a (non-informative) Jeffreys prior. These data must be generated by a separate survey effort typically involving observation of telemetered tortoises to monitor daily activity patterns during the survey period. Non-detection may be due to shelter that obscures the individual (e.g., burrow, vegetation), coloration, ground texture, or other factors. In the absence of data applicable to a specific survey effort, other means of estimating g_0 must be employed.

2.3.5. Determination of g_m

The quantity g_m refers to the probability that a tortoise present and visible in a photograph will be detected by the computer vision object detection system. In practice, this is the same as the recall value of the trained CNN model as determined by model validation procedures. This value is a property of the trained CNN itself and is not related to the distance from the center of the photograph or to visual impediments. It is therefore distinct from g_r and g_0.

2.3.6. Estimate the Population, Density, and Abundance

The population (N) is estimated via a two-stage process of 1) estimating the detection function, and 2) estimating the total population given the detection probabilities (Madsen et al. 2020; Dalthorp et al. 2018). Finally, the tortoise density within the study area is estimated as $\widehat{D} = \frac{N}{A}$ where A is the area photographed. A is determined in a GIS environment by performing a vector dissolve operation on the photo polygons and measuring the area of the resulting survey area polygon. Abundance is then calculated as the product of $\widehat{D}$ and the total area of the project site.

3. Controlled Test to Derive Detection Curve

A controlled field test was conducted in order to generate a detection curve using the drone platform and camera employed in the 2025 BCCE surveys. This test consisted of drone surveys of the U.S. Fish and Wildlife Survey's (USFWS) training arena located outside of Las Vegas, NV. The arena is used by USFWS and its contractors to train pedestrian survey crews participating in its ongoing desert tortoise range-wide monitoring program. It also serves to establish baseline detection curves for each of these survey teams to be used in the USFWS's established line distance survey protocol. It consists of 12 parallel linear transects marked by posts and spaced at 25 meter intervals. A large number of tortoise surrogates ("styrotorts") are placed at random locations in the vicinity of these transect lines and are used to teach survey methods and measure the effectiveness of the pedestrian survey teams. The sample available for detection consisted of 144 adult tortoise surrogates. This same arena was flown in 2022 using a different set of equipment and methods (Bandy 2022), and the results of the 2025 test will be compared to the results of the 2022 tests.

3.1. Drone flights and tortoise detection

The drone surveys of the USFWS training arena were conducted on April 19, 2025. The entire arena area was flown at 73 meters flight elevation and terrain following techniques were used to maintain a constant elevation above ground level. Equipment, software, and methods were the same as those employed in the 2025 BCCE surveys. The collected photographs were processed by Resi's tortoise detection model and the detections were reviewed and confirmed by a trained human observer. The resulting dataset included 118 unique adult tortoise surrogate detections. The detection rate was 82% for adult tortoise surrogates (118/144).

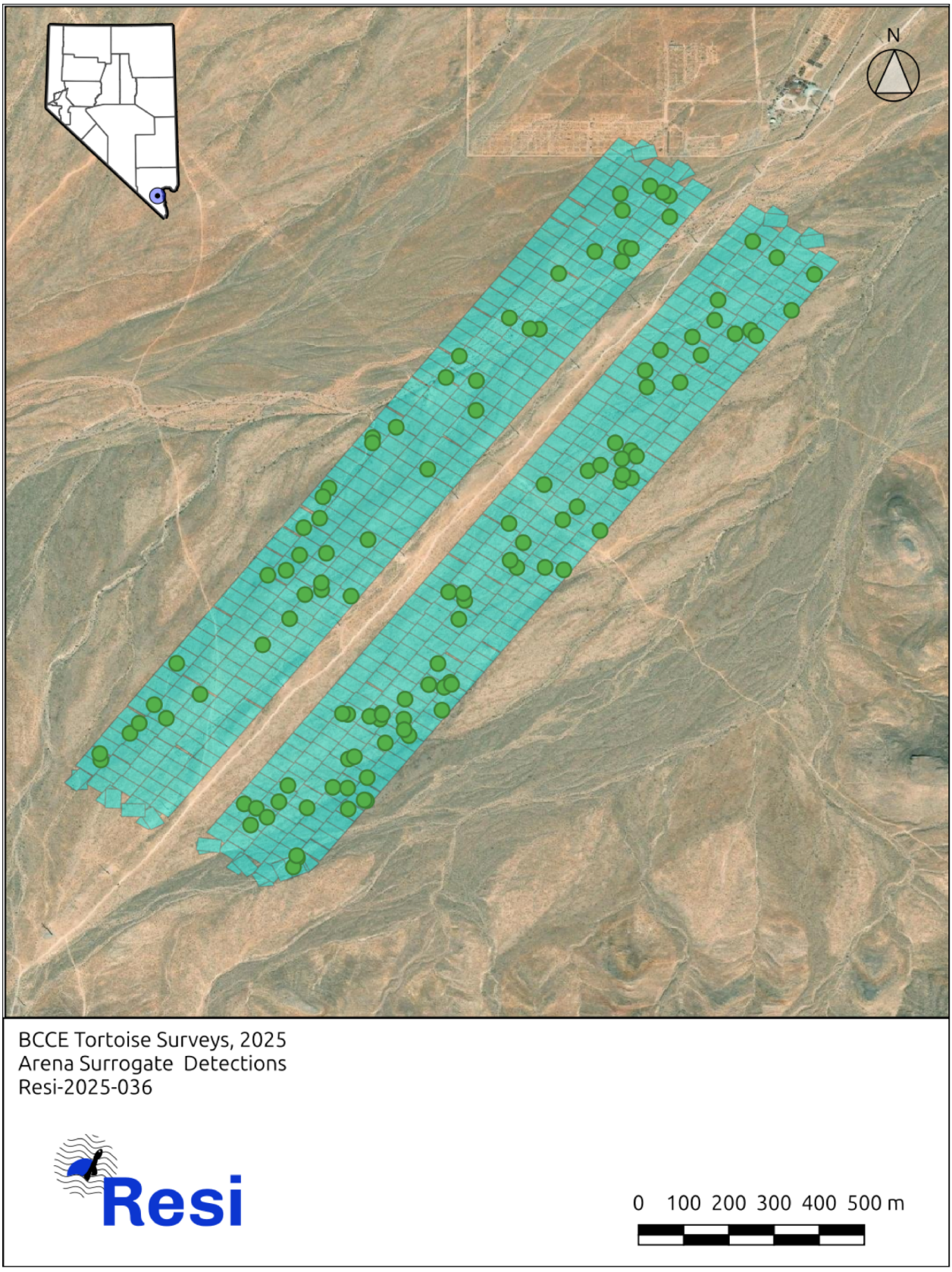

Figure 3.1. Training arena photos and adult detections: 118/144=82%.

3.2. Distance Analysis

3.2.1. Fit the Distance Model $g(r)$

The total sample of tortoise surrogate detections available for fitting a detection curve included 123 adults.[1] A half-normal model was fitted to the adult surrogate sample, as described on page 10 (Figure 3.2). The fitted curve equates to a mean detection probability across a single photograph of 85%, as compared to 74% for the 2022 test. The curves (Figure 3.2) show that detection falls off much more quickly with distance from the center of the photograph for the 2022 test than for the 2025 test.

3.2.2. Combine g_0, g_m, and g_r into Estimated Overall Detection Rate $\hat{g}$

In the case of the training arena, no tortoises were placed in burrows or were otherwise made unavailable for drone observation. It is therefore the case that $g_0 = 1$, as distance sampling conventionally assumes.

The quantity g_m is a property of Resi's trained CNN object detection model and is determined by evaluation of a separate validation sample segregated during model training. The validation sample employed in this study contained 118 randomly selected adult tortoise images. The model recall of this sample was 89.0% (105/118), so in this analysis $g_m = 0.89$.

The quantity g_r is estimated from the fitted distance model $g(r)$ and the photo polygons as described on page 10. Also, it is worth observing that since $g_0 = 1$ and $g_m = 1$, in the special case of surveying for tortoise surrogates in the USFWS training arena $\hat{g} = \hat{g}_r$. For adult tortoise surrogates, mean $\hat{g}$ for the 2025 test is 87%. This is significantly higher than the 81% value observed in the 2022 test, and also somewhat higher than the measured detection rate of 82%.

3.2.3. Estimate Total Population N

The total estimated population of adult tortoise surrogates in the covered area, as determined by DRONEDISTANCE, is 151 with a 90% confidence interval of 133-171. (Figure 3.4). This mean estimated N value is consistent with the known population number of 144, with an error rate of approximately 4.8%, and the known value is well within the calculated confidence interval.

[1] This number includes duplicate detections of certain surrogates in multiple photos.

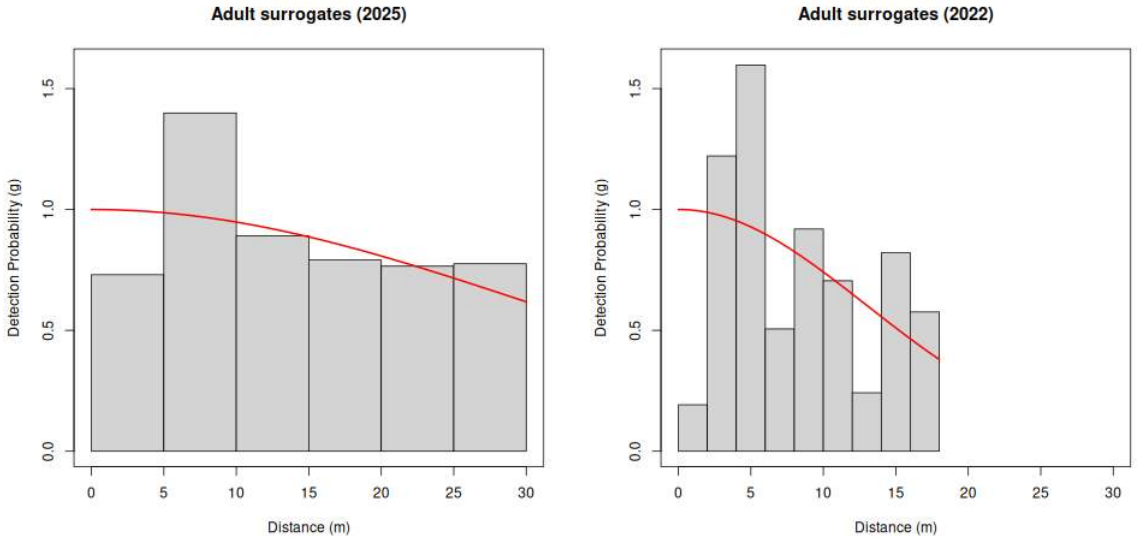

Figure 3.2. Half-normal distance model fitted to training arena observations of adult tortoise surrogates: 2025 (left; $I = 5.345e{-}4, AIC = 249.3$) vs 2022 (right; $I = 2.989e{-}3, AIC = 534.9$)

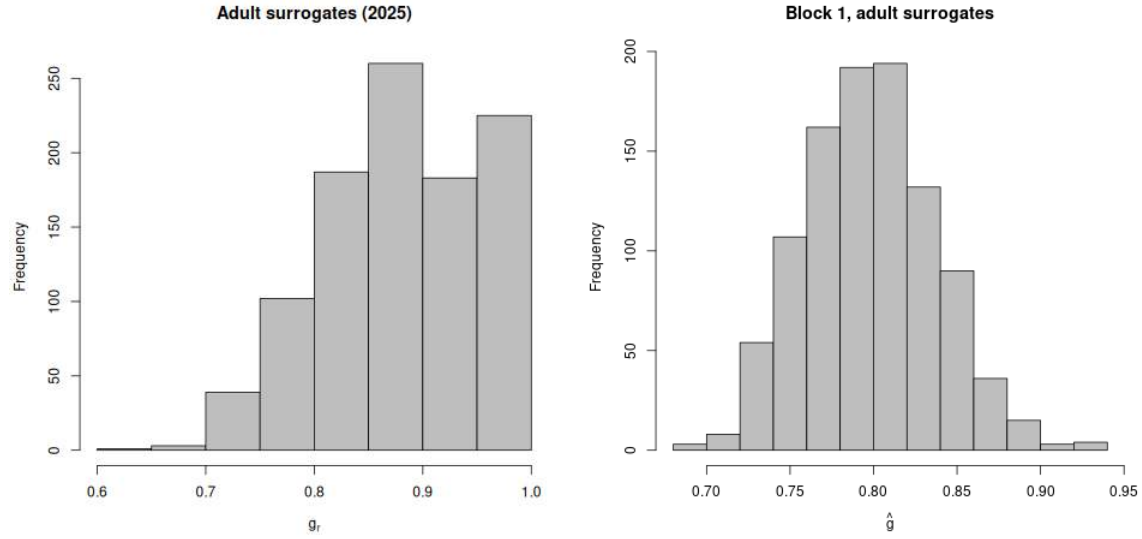

Figure 3.3. Estimated $\hat{g}$ adult tortoise surrogates: 2025 (left) vs 2022 (right)

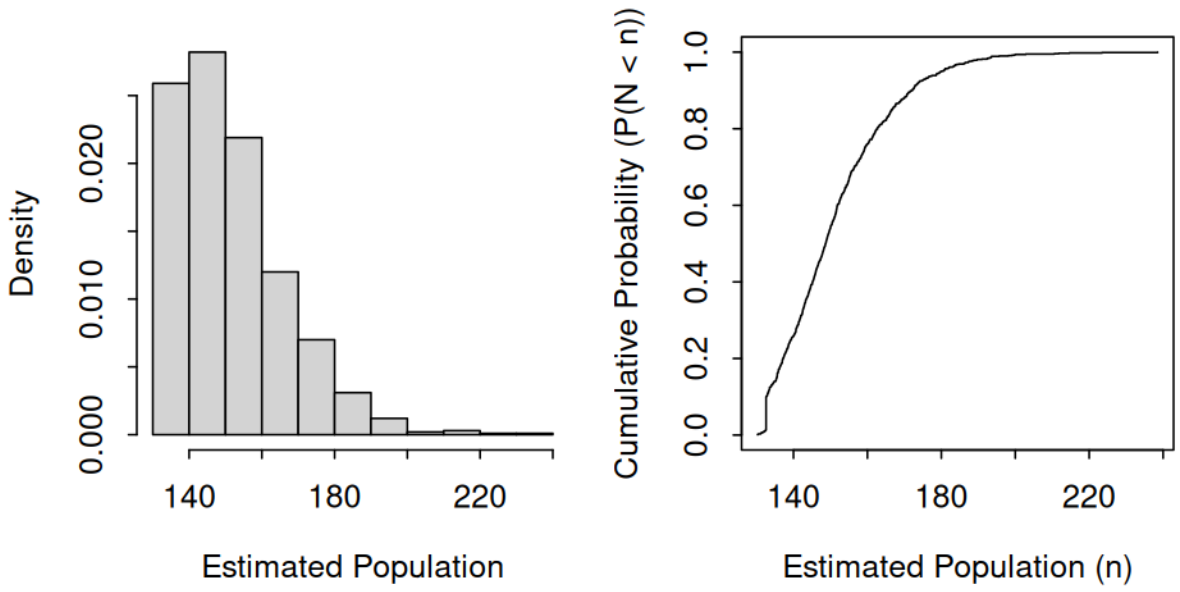

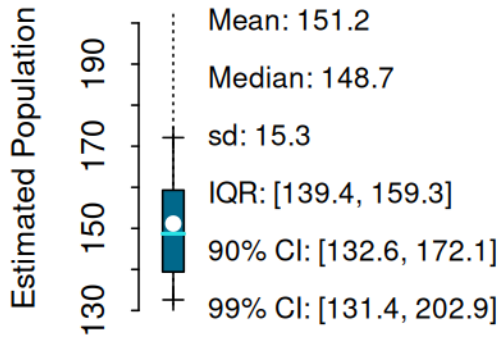

Figure 3.4. Estimated N, adult tortoise surrogates

3.3. Discussion

The drone survey method performed well in the context of the USFWS training arena - 82% of adult tortoise surrogates were detected. This compares to 81% of surrogates detected in the 2022 arena surveys. This study has confirmed that the drone method is superior to pedestrian methods at detecting tortoise surrogates when they are above ground and not obscured by vegetation. Figure 3.5 shows the 2025 and 2022 drone survey detection curves for adult surrogates derived from the USFWS arena data and compares these to detection curves for pedestrian surveyors. The single observer pedestrian curve was fitted from data reported by USFWS (2009: 4-14), and the double observer pedestrian curve was fitted using data collected during 2022 surveys in Washington County, Utah (Bandy and Rognan 2022, cf. U.S. Fish and Wildlife Service 2020: 24 for similar and comparable data). As previously discussed, the 2025 drone survey method resulted in the detection of 82% of adult tortoise surrogates. Extrapolating from the detection curves in Figure 3.5, in order to achieve a comparable detection rate over a given area of interest the double observer pedestrian method would require a transect width of 16 meters, while the single pass pedestrian method would require a transect width of 6 meters (Table 3.1).

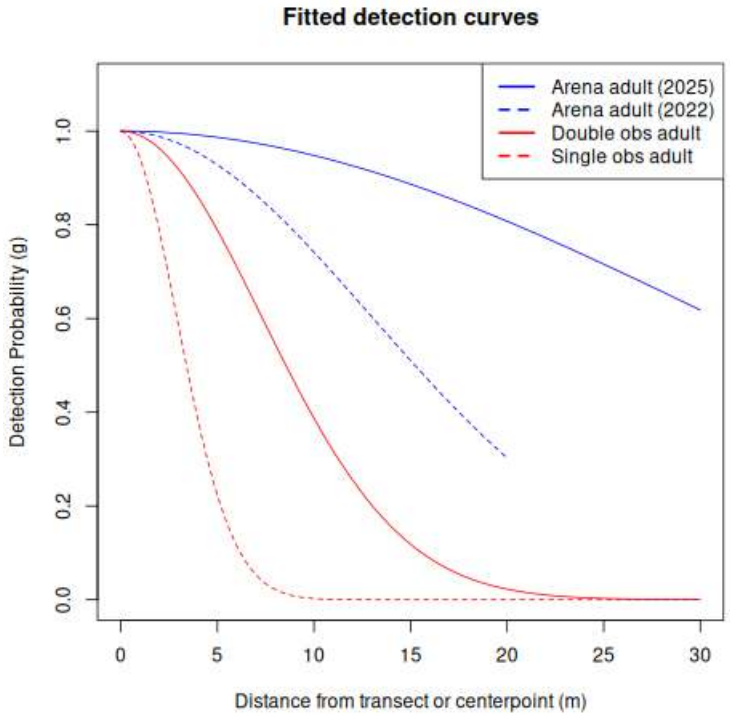

Figure 3.5. Detections curves: drone and pedestrian survey methods

In terms of adult tortoise surrogate detection, the drone method's detection rate is about 82%, at least when flown using the 2025 methods. This detection rate is achievable by pedestrian methods only at a very high spatial intensity and low efficiency. At this detection rate, the 2022 drone method is approximately 16-21x more efficient than pedestrian methods in terms of field time, while the 2025 drone method is 40-54x more efficient.

	Transect Width	Acres/person-hour
Single Observer	6	3
Double Observer	16	4
Drone (2022)	30	63
Drone (2025)	52	162

Table 3.1. Survey methods compared in terms of transect width (meters) required to achieve an adult tortoise surrogate detection rate ($\hat{g}$) of $> 80\%$ and corresponding efficiency (acres/person-hour)

Resi's statistical methods for density and abundance estimation also performed well. Distance analysis using the DRONEDISTANCE R package produced abundance estimates for adult tortoise surrogates within 6% of known counts. These results are comparable to the results of the 2022 arena drone survey tests. The detection curve generated as a result of the 2025 USFWS arena flights can be used in other survey projects in similar environments, such as the BCCE.

4. Results of the BCCE Surveys

4.1. Baseline g_0 Telemetry Data

Throughout the period in which drone flights took place, the Great Basin Institute (GBI) was continuously conducting a telemetry study of desert tortoises within the BCCE. The study began in February and continued throughout the time of the drone survey and later. Tortoises were regularly observed active and above ground beginning on May 4. GBI biologists made a total of 134 observations of 29 individual tortoises between April 19 and May 10, when drone flights ended. These data were used to estimate above ground activity and tortoise detectability (g_0) during the survey period.

Tortoises were mainly in their burrows during the first two survey periods. While they were largely detectable by pedestrian surveyors, they were almost entirely undetectable by drone surveys (Table 4.1). While relatively few tortoises were available for detection even in the third survey period, g_0 rose as high as 0.2. This value of g_0, though higher than the first two survey periods, was still extraordinarily low compared to other measured and estimated values for drone surveys (Table 4.2). This very low g_0 value is likely related to

	Drone Detectability (g_0)	Pedestrian Detectability (g_0)	Dates	Num Observations	Drone Survey Days
Period 1	3%	67%	4/10-4/22	39	5
Period 2	5%	61%	4/23-5/4	56	5
Period 3	20%	82%	5/6-5/10	22	5

Table 4.1. Percent of telemetered tortoises visible (g_0) by survey period and method

Red Cliffs Desert Reserve 2023	0.73
Red Cliffs Desert Reserve 2025	0.18
BCCE 2024	0.45

Table 4.2. Measured drone survey g_0 values

extreme drought conditions in southern Nevada in the Spring of 2025. It is worth noting

that measured g_0 was even lower (0.18) in southwestern Utah in the same period. For this reason, only survey period 3 data is used for population estimation in the current study. The measured value of $g_0 = 0.2$ is employed in the analysis that follows.

4.2. Drone Surveys

Drone surveys for the desert tortoise were completed between two hours after sunrise and 1 PM between March 15 and May 10, 2025. They resulted in the detection of ten adult tortoises (Midline Carapace Length [MCL] >= 180 mm), five juveniles, and ten tortoise carcasses (Figure 4.1).

4.3. Distance Analysis

Distance analysis was performed using the DRONEDISTANCE R package, described above. Since ten detections is not adequate to fit a detection curve, a function was employed that was fitted using 123 drone/AI detections of adult-sized tortoise surrogates from the USFWS arena trials described in Chapter 3 (Figure 4.2).

4.3.1. Estimate g_0

The quantity g_0 is estimated from the surface activity observations dataset described on page 20. The mean value employed will be 0.2 (Figure 4.3). As noted, this is a very low value reflecting low tortoise detectability due to severe drought conditions.

4.3.2. Combine $\hat{g}_0$, g_m and $\hat{g}_r$ into Estimated Overall Detection $\hat{g}$

The quantity g_r is estimated from the fitted distance model $g(r)$ and the drone photo polygons as described above and in Bandy (2022). It varies from one survey location to another due to the degree and configuration of photo overlap. In general, the higher the degree of photographic overlap in a dataset, the higher the overall detection probability will be. For the current study, mean $\hat{g}_r$ is estimated to be 0.88 (Figure 4.4).

The quantity g_m is a property of Resi's trained CNN object detection model and is determined by evaluation of a separate validation sample segregated during model training. The validation sample employed in this study contained 118 randomly selected adult tortoise

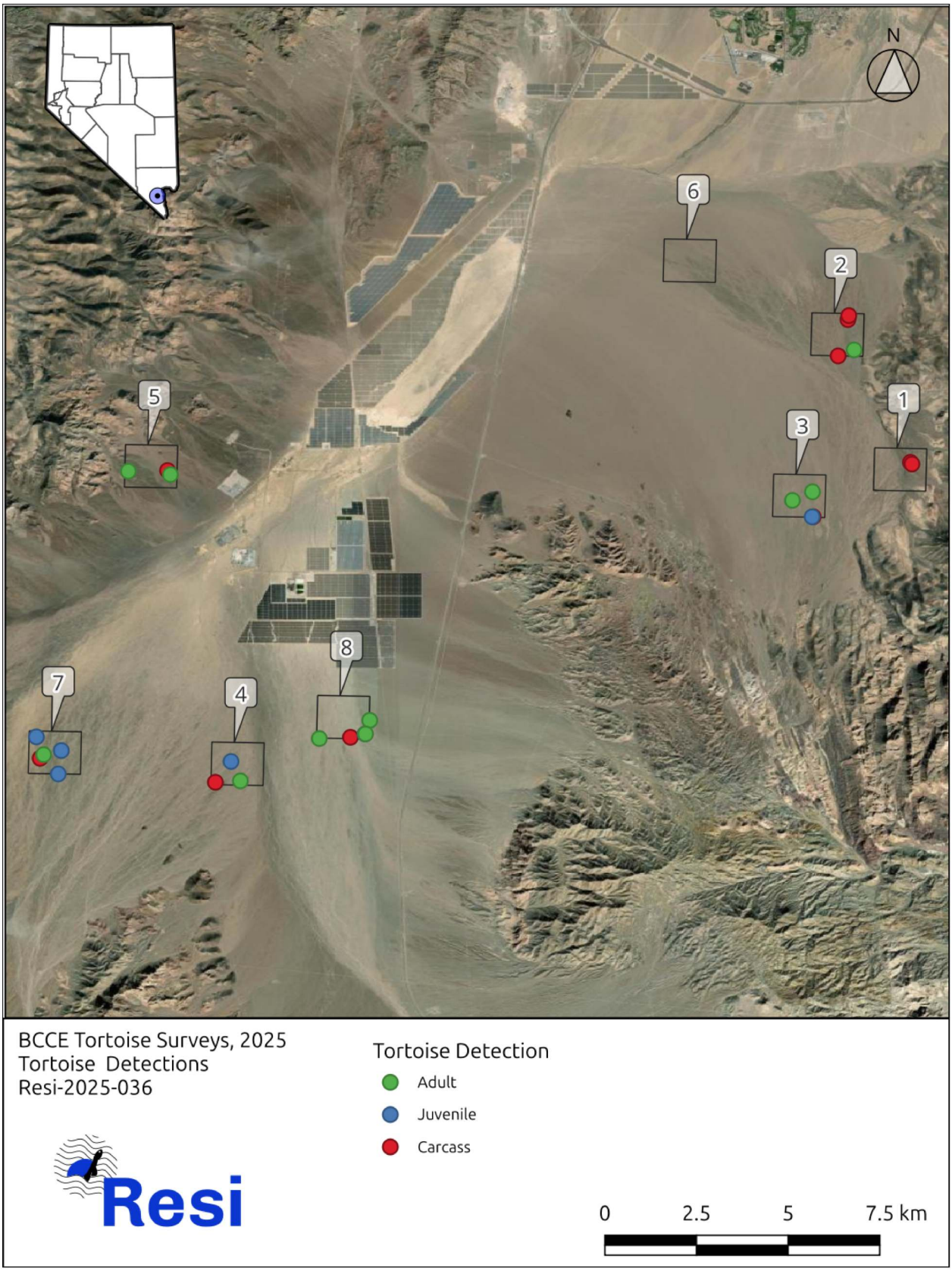

Figure 4.1. Tortoise detections

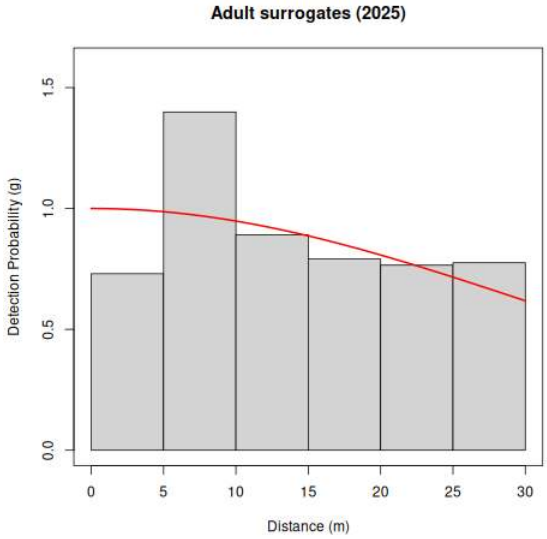

Figure 4.2. Half-normal distance model fitted to adult-sized tortoise surrogate detections ($I = 5.345e{-}4, AIC = 249.3$)

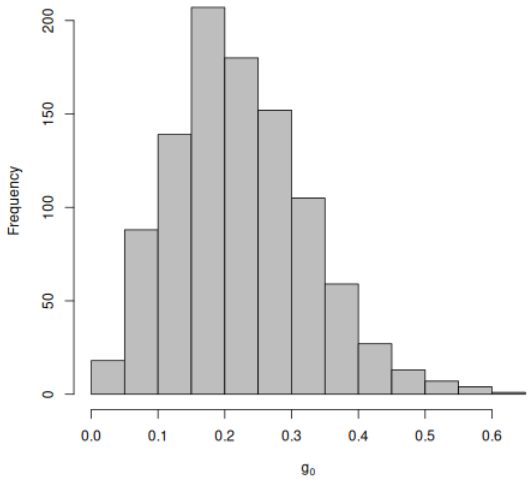

Figure 4.3. g_0, adult tortoises, survey period 3

images. The model recall of this sample was 89.0% (105/118), so in this analysis $g_m = 0.89$. Again, this applies only to adult tortoises since data to confidently derive a g_m value for juveniles are not available.

The quantity $\hat{g}$ is an estimate of the tortoise detection probability throughout the entire aerial photographic dataset. It is calculated as the product of $\hat{g}_0$, g_m, and $\hat{g}_r$. For the current study, mean $\hat{g}$ is 0.16, meaning that we expect to detect approximately 16% of tortoises in the survey area using the drone/AI method. This is very low compared to other recent applications of the method, due mainly to the unusually low value of g_0 calculated for this survey period and despite a quite high value of $\hat{g}_r$.

4.3.3. Estimate Total Population N

N is the number of tortoises present in the photographed area (Figure 4.5). It is estimated from the number of detections and from $\hat{g}$ using the method described above and in Bandy (2022: 9-10). For the current study, the total population within the survey period 3 photographed area is estimated to be 48 with a 90% confidence interval of 38-57.

4.3.4. Density and Abundance

Density is calculated by dividing N by the photographed area of each dataset. The photographed area is normally calculated in a GIS environment by performing a vector dissolve operation on the photo polygons and measuring the area of the resulting survey area polygon. However, this calculation was complicated by the fact that the Spring of 2025 was abnormally cold followed a very dry winter. As noted above, tortoise detectability was extremely low during the first two survey periods. [1] Tortoises were more detectable in the third survey period, and only data from that time will be used for density and abundance estimation. Areas photographed prior to that time should not be included in the total photographed area. A total of 4,079.5 acres (16.51 km^2) were flown during the third survey period, so that number is used as the photographed area in this analysis.

The mean estimated density of desert tortoises within the photographed area is 2.9/km^2 with a 90% confidence interval between 2.3/km^2 and 3.5/km^2. Abundance is calculated by multiplying the density by the total project area (Table 4.3). The desert tortoise abundance within the 86,430-acre conservation easement is estimated to be 1025 with a 90% confidence

[1] Incidentally, Mojave Max did not emerge until May 8, late in the third survey period. This is the latest emergence ever documented by the Mojave Max outreach program.

interval of 825-1219. The surveyed area represents approximately 4.7% of the entire BCCE.

N	km^2 Sampled	Density (N/km^2)	km^2 Total	Abundance
48 [38, 57]	16.51	2.9 [2.3, 3.5]	349.8	1025 [825, 1219]

Table 4.3. Density and abundance estimates with 90% confidence intervals.

4.4. Tortoise Burrows

While the primary goal of the drone surveys was to estimate density and abundance of tortoises, data on burrows was also collected. A neural network was trained to detect burrows based on tagged images of 509 tortoise burrows from Resi's library. These were primarily Mojave desert tortoise burrow images collected from sites in California (n=194), Nevada (n=157), and Utah (n=55). Some images of Bolsón tortoise (*Gopherus flavomarginatus*) burrows were also included (n=103), as well as 251 landscape images that did not contain any tortoise burrows. The trained model was effective, with a recall of approximately 0.82 and a precision of approximately 0.67 based on the validation dataset. As with tortoise detections, all burrow detections were reviewed in order to eliminate false positives and were classified as best as possible using the same schema employed in the USFWS pre-project survey protocol (U.S. Fish and Wildlife Service 2009).

A total of of 50 class 1 and 2 soil burrows were detected (Figure 4.7). The distribution of the burrows is broadly consistent with tortoise detections.

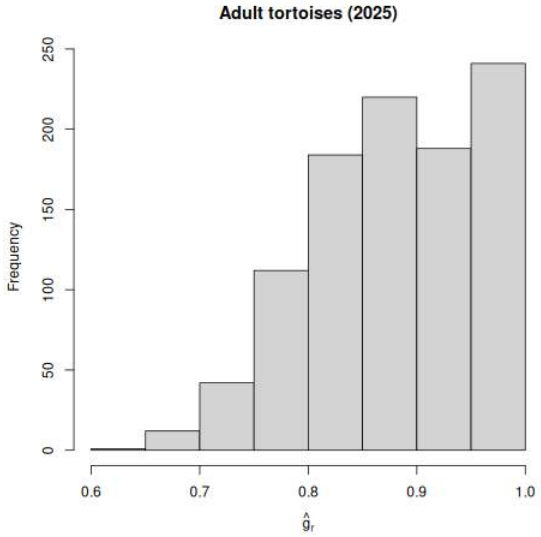

Figure 4.4. $\hat{g}_r$, adult tortoises, survey period 3

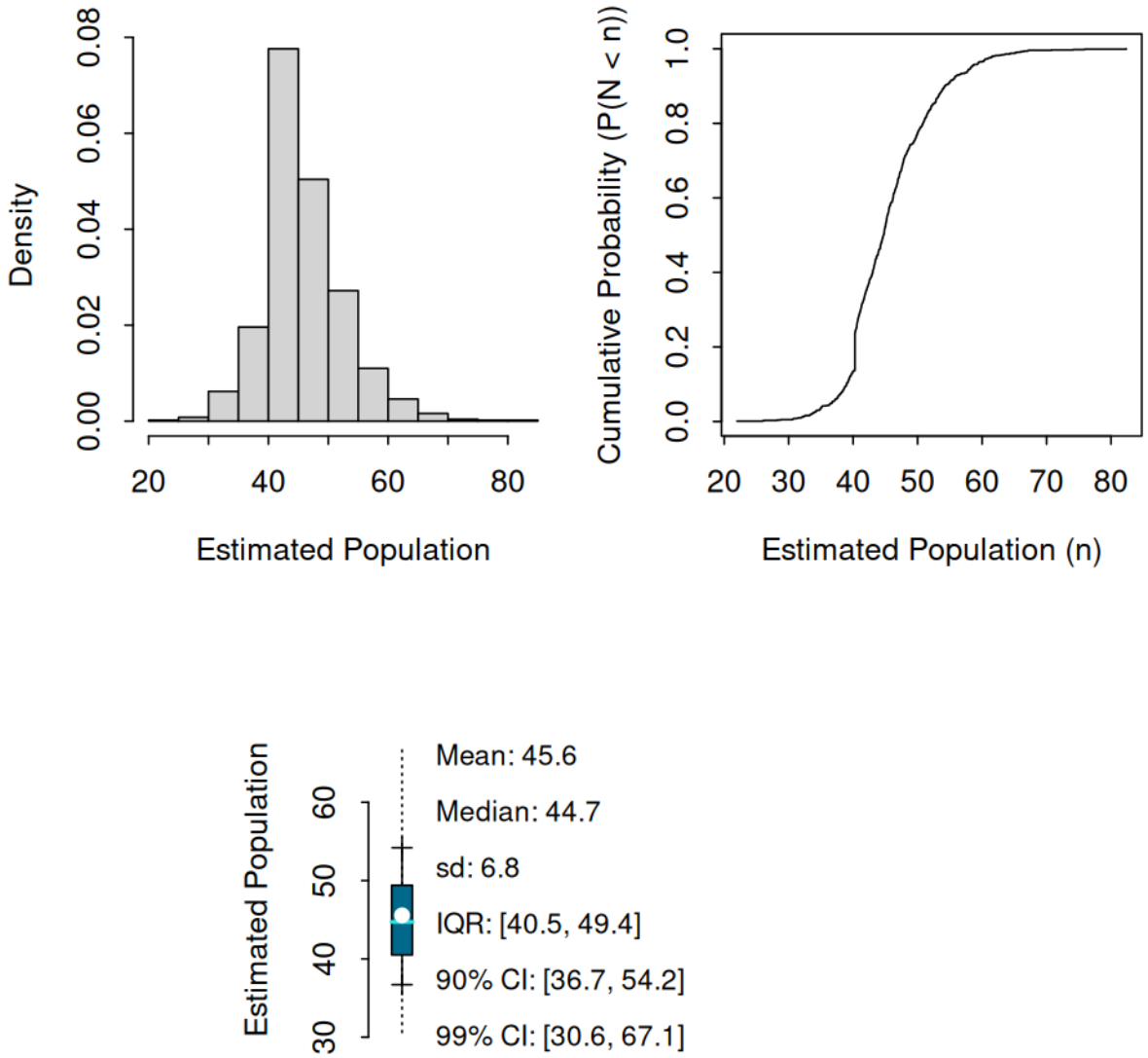

Figure 4.5. Estimated N, adult tortoises

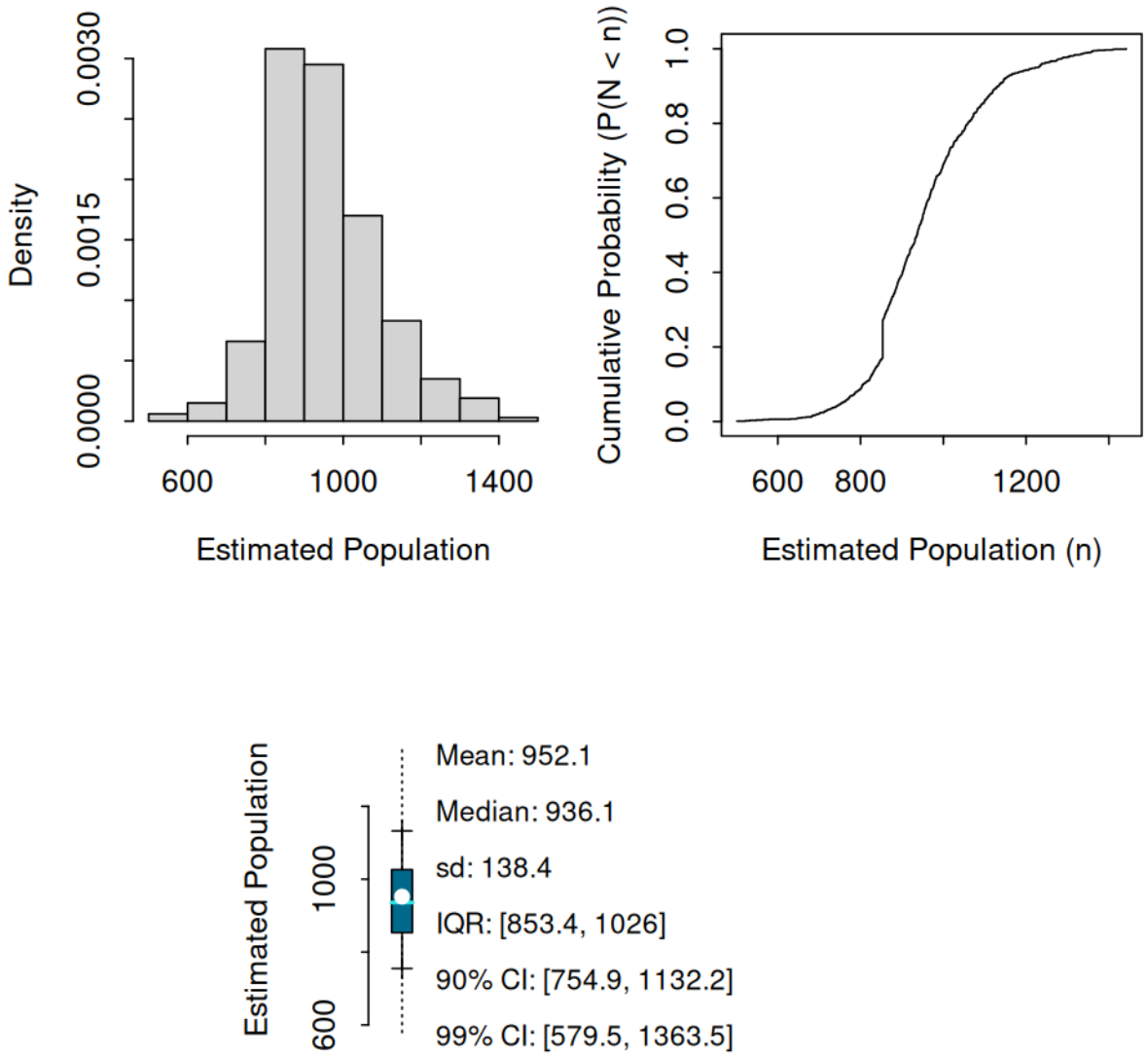

Figure 4.6. Estimated BCCE abundance, adult tortoises

Figure 4.7. Burrow detections

5. Conclusion and Recommendations

The drone/AI survey method was successful in detecting tortoises and burrows in the BCCE. This study has used distance sampling methods to estimate an easement-wide tortoise abundance of 1025 [825,1219]. This is based on a 4.7% sample of the total area of the BCCE. The estimated population density of 2.9 tortoises/km^2 is comparable to reported densities for this portion of the Mojave. For example, the nearby Ivanpah Valley Tortoise Conservation Area (TCA) had a density of 2.8 tortoises/km^2 in 2012 and 2.6 tortoises/km^2 in 2019, while the Eldorado Valley TCA had a density of 0.9 tortoises/km^2 in 2012 and 2.3 tortoises/km^2 in 2019 (Allison and McLuckie 2018; U.S. Fish and Wildlife Service 2020).

The estimated density is also significantly lower than the density estimated in the 2024 BCCE surveys (4.6 tortoises/km^2; Bandy 2024b). However, that estimate was based on a smaller number of detections and a much smaller surveyed space. As a consequence, it had very wide confidence intervals. This current estimate falls well above the lower bound of the 2024 study's 90% confidence interval (2.1 tortoises/km^2). The two estimates are therefore compatible.

As was also the case in the 2024 survey, a significant amount of survey effort was wasted due to low tortoise detectability in the early part of the survey period (Bandy 2024b). If the survey effort had begun on or shortly after May 1, it is likely that thirty or more tortoises would have been detected and the density and abundance estimates presented here would have been based on better data and likely would have had narrower confidence intervals. In the future, it will be critical to establish improved communication between the drone survey team and the telemetry monitoring teams so that drone surveys do not begin before significant above-ground tortoise activity has been observed in the study area.

Literature Cited

Allison, L. J. and McLuckie, A. M. (2018). Population trends in Mojave desert tortoises (Gopherus agassizii). *Herpetological Conservation and Biology*, 13(2):433–452.

Augustine, J. K. and Burchfield, D. (2022). Evaluation of unmanned aerial vehicles for surveys of lek-mating grouse. *Wildlife Society Bulletin*, 46(4):e1333.

Bandy, M. (2021). Surveying for Desert Tortoises using Drones and Artificial Intelligence: A Pilot Study. Technical report 2021-001-01, Resi Solutions.

Bandy, M. (2022). A Method for Mojave Desert Tortoise Drone Surveys and a Controlled Field Test. Technical report 2022-001-02, Resi Solutions.

Bandy, M. (2023). Drone Surveys for the Mojave Desert Tortoise in Zones 2-5 of the Red Cliffs Desert Reserve. Technical report 2023-014-01, Resi Solutions.

Bandy, M. (2024a). An AI-Assisted Drone Survey for Mojave Desert Tortoises within the Bonanza Solar Project Area, Clark County, NV. Technical report 2024-057-01, Resi Solutions.

Bandy, M. (2024b). An AI-Assisted Drone Survey for Mojave Desert Tortoises within the Boulder City Conservation Easement, Clark County, NV. Technical report 2024-015-01, Resi Solutions.

Bandy, M. and Rognan, C. (2022). Drone and Pedestrian Desert Tortoise Surveys in Zone 6 of the Red Cliffs Desert Reserve. Technical report 2022-001-01, Resi Solutions.

Buckland, S. T., Anderson, D. R., Burnham, K. P., Laake, J. L., Borchers, D. L., and Thomas, L. (2001). *Introduction to distance sampling: estimating abundance of biological populations*. Oxford University Press.

Christie, K. S., Gilbert, S. L., Brown, C. L., Hatfield, M., and Hanson, L. (2016). Unmanned aircraft systems in wildlife research: current and future applications of a transformative technology. *Frontiers in Ecology and the Environment*, 14(5):241–251. _eprint: https://esajournals.onlinelibrary.wiley.com/doi/pdf/10.1002/fee.1281.

Dalthorp, D., Madsen, L., Huso, M. M., Rabie, P. A., Wolpert, R., Studyvin, J., Simonis, J., and Mintz, J. (2018). GenEst statistical models - A generalized estimator of mortality. Technical report, US Geological Survey. ISSN: 2328-7055.

Delplanque, A., Foucher, S., Lejeune, P., Linchant, J., and ThÃ©au, J. (2021). Multispecies detection and identification of African mammals in aerial imagery using convolutional neural networks. *Remote Sensing in Ecology and Conservation*. Publisher: Wiley Online Library.

Elmore, J. A., Curran, M. F., Evans, K. O., Samiappan, S., Zhou, M., Pfeiffer, M. B., Blackwell, B. F., and Iglay, R. B. (2021). Evidence on the effectiveness of small unmanned aircraft systems (sUAS) as a survey tool for North American terrestrial, vertebrate animals: a systematic map protocol. *Environmental Evidence*, 10(1):1–6. Publisher: BMC.

Huerta, J. O., Henke, S. E., Perotto-Baldivieso, H. L., Wester, D. B., and Page, M. T. (2020). Ability of Observers to Detect Herpetofaunal Models Using Video from Unmanned Aerial Vehicles. *Herpetological Review*, 51(1):11–17.

Hyun, C.-U., Park, M., and Lee, W. Y. (2020). Remotely Piloted Aircraft System (RPAS)-Based Wildlife Detection: A Review and Case Studies in Maritime Antarctica. *Animals*, 10(2387):2387. Publisher: MDPI AG.

Inman, V. L., Kingsford, R. T., Chase, M. J., and Leggett, K. E. A. (2019). Drone-based effective counting and ageing of hippopotamus (Hippopotamus amphibius) in the Okavango Delta in Botswana. *bioRxiv*. Publisher: Cold Spring Harbor Laboratory _eprint: https://www.biorxiv.org/content/early/2019/07/01/689059.full.pdf.

Jones, G. P., Pearlstine, L. G., and Percival, H. F. (2006). An Assessment of Small Unmanned Aerial Vehicles for Wildlife Research. *Wildlife Society Bulletin*, 34(3):750–758. _eprint: https://onlinelibrary.wiley.com/doi/pdf/10.2193/0091-7648%282006%2934%5B750%3AAAOSUA%5D2.0.CO%3B2.

Linchant, J., Lhoest, S., Quevauvillers, S., Lejeune, P., Vermeulen, C., Ngabinzeke, J. S., Belanganayi, B. L., Delvingt, W., and BouchÃ©, P. (2018). UAS imagery reveals new survey opportunities for counting hippos. *PLoS ONE*, 13(11):e0206413. Publisher: Public Library of Science (PLoS).

Madsen, L., Dalthorp, D., Huso, M. M. P., and Aderman, A. (2020). Estimating population size with imperfect detection using a parametric bootstrap. *Environmetrics*, 31(3):e2603. Publisher: Wiley Online Library.

Miller, D. L., Burt, M. L., Rexstad, E. A., and Thomas, L. (2013). Spatial models for distance sampling data: recent developments and future directions. *Methods in Ecology and Evolution*, 4(11):1001–1010. _eprint: https://besjournals.onlinelibrary.wiley.com/doi/pdf/10.1111/2041-210X.12105.

Miller, D. L., Rexstad, E., Thomas, L., Marshall, L., and Laake, J. L. (2017). Distance Sampling in R. *bioRxiv*. Publisher: Cold Spring Harbor Laboratory _eprint: https://www.biorxiv.org/content/early/2017/11/28/063891.full.pdf.

Paszke, A., Gross, S., Massa, F., Lerer, A., Bradbury, J., Chanan, G., Killeen, T., Lin, Z., Gimelshein, N., Antiga, L., Desmaison, A., Kopf, A., Yang, E., DeVito, Z., Raison, M., Tejani, A., Chilamkurthy, S., Steiner, B., Fang, L., Bai, J., and Chintala, S. (2019). PyTorch: An Imperative Style, High-Performance Deep Learning Library. In *Advances in Neural Information Processing Systems 32*, pages 8024–8035. Curran Associates, Inc.

Ramos, E. A., Ramos, E. A., Maloney, B., Maloney, B., Magnasco, M. O., Reiss, D., and Reiss, D. (2018). Bottlenose Dolphins and Antillean Manatees Respond to Small Multi-Rotor Unmanned Aerial Systems. *Frontiers in Marine Science*, 5. Publisher: Frontiers Media S.A.

Thomas, L., Buckland, S. T., Rexstad, E. A., Laake, J. L., Strindberg, S., Hedley, S. L., Bishop, J. R., Marques, T. A., and Burnham, K. P. (2010). Distance software: design and analysis of distance sampling surveys for estimating population size. *Journal of Applied Ecology*, 47(1):5–14. _eprint: https://besjournals.onlinelibrary.wiley.com/doi/pdf/10.1111/j.1365-2664.2009.01737.x.

U.S. Fish and Wildlife Service (2009). *Desert Tortoise (Mojave Population) Field Manual (Gopherus agassizii)*. Region 8, Sacramento, California.

U.S. Fish and Wildlife Service (2020). Range-Wide Monitoring of the Mojave Desert Tortoise (Gopherus Agassizii): 2019 Annual Reporting. Technical report, Desert Tortoise Recovery Office, Reno, Nevada.

Watts, A. C., Bowman, W. S., Abd-Elrahman, A. H., Mohamed, A., Wilkinson, B. E., Perry, J., Kaddoura, Y. O., and Lee, K. (2008). Unmanned Aircraft Systems (UASs) for Ecological Research and Natural-Resource Monitoring (Florida). *Ecological Restoration*, 26(1):13–14. _eprint: http://er.uwpress.org/content/26/1/13.full.pdf+html.

Zhou, M., Elmore, J. A., Samiappan, S., Evans, K. O., Pfeiffer, M. B., Blackwell, B. F., and Iglay, R. B. (2021). Improving Animal Monitoring Using Small Unmanned Aircraft

Systems (sUAS) and Deep Learning Networks. *Sensors*, 21(5697):5697. Publisher: MDPI AG.

Appendix A.

Survey Effort by Plot and Date

Table A.1. Survey effort summary by plot and date

Round	Date	Plot	Photo count	Photographed acres
1	2025-04-15	1	1271	507.1
1	2025-04-20	2	1281	511.5
1	2025-04-16	3	1297	512.7
1	2025-04-22	4	1286	509.8
1	2025-04-21	5	1297	514.1
1	2025-04-15	6	1439	513.3
1	2025-04-22	7	1357	510.2
1	2025-04-21	8	1276	505.6
2	2025-04-24	1	1283	511.6
2	2025-04-23	2	1324	514.5
2	2025-04-25	3	1296	512.2
2	2025-05-03	4	1285	509.5
2	2025-05-04	5	1294	510.8
2	2025-04-24	6	1274	502.3
2	2025-05-03	7	1283	505.6
2	2025-04-28	8	1279	503.0
3	2025-05-06	1	1299	510.3
3	2025-05-07	2	1309	514.0
3	2025-05-06	3	1281	511.1
3	2025-05-08	4	1273	508.2
3	2025-05-10	5	1296	511.4
3	2025-05-07	6	1284	508.8

Table A.1. Survey effort summary by plot and date

Round	Date	Plot	Photo count	Photographed acres
3	2025-05-09	7	1286	512.0
3	2025-05-08	8	1277	505.3